IOP Publishing Measurement Science and Technology

Meas. Sci. Technol. **18** (2007) 1811–1817 doi:10.1088/0957-0233/18/7/003

Simultaneous measurement of acoustic and streaming velocities using synchronized PIV technique

Majid Nabavi, M H Kamran Siddiqui and Javad Dargahi

Department of Mechanical and Industrial Engineering, Concordia University, 1455 de Maisonneuve Blvd West, Montreal, Quebec, H3G 1M8, Canada

E-mail: siddiqui@encs.concordia.ca

Received 23 November 2006, in final form 13 March 2007
Published 9 May 2007
Online at stacks.iop.org/MST/18/1811

Abstract

Synchronized particle image velocimetry (PIV) technique has been applied to measure the acoustic and streaming velocity fields simultaneously, inside a standing-wave rectangular channel. In this technique, the velocity fields were sampled at a certain phase of the excitation waveform. The acoustic velocity fields were obtained by cross-correlating the two consecutive PIV images, whereas the streaming velocity fields were obtained by cross-correlating the alternative PIV images at the same phase. The experimental values of the mean acoustic velocity and RMS streaming velocities obtained from PIV are in good agreement with the theoretical values, showing that this novel approach can measure both acoustic and streaming velocities, accurately and simultaneously, in the presence of large amplitude acoustic wave.

Keywords: acoustic streaming, particle image velocimetry, acoustic standing wave

1. Introduction

Acoustic streaming is a stationary fluid flow generated by sound. Among different types of acoustic streaming, Rayleigh streaming or outer streaming is always associated with a standing-wave resonator. Rayleigh streaming is a vortex-like structure generated outside the boundary layer in a standing-wave resonator. The interaction between the acoustic waves in viscous fluids and solid boundaries is responsible for this kind of streaming. Vortex motion generated inside the boundary layer is called Schlichting or inner streaming [1].

Although the phenomenon of acoustic streaming is well known, relatively few experimental investigations have been performed to measure the acoustic streaming velocity fields inside a standing-wave resonator. Arroyo and Greated [2] used a stereoscopic PIV to measure all three components of the streaming velocity field. They generated a standing wave of 18 cm length inside a 62.5 cm long tube. They, however, measured the streaming velocity field only in a region within 2 cm around the velocity node. Hann and Greated [3] measured two components of both acoustic and streaming velocity fields simultaneously in the vicinity of a velocity node (in a 2 cm band around the node) in a 70 cm long resonator excited by a 1616 Hz sinusoidal signal. Campbell *et al* [4] also reported PIV measurements of streaming velocity fields in a cylindrical resonator in the vicinity of a velocity node. The only experimental study that reported simultaneous measurement of acoustic and streaming velocities at different locations along a resonator is by Thompson *et al* [5]. They used laser Doppler anemometry (LDA) with burst spectrum analysis (BSA) to study the acoustic streaming generated in a cylindrical standing-wave resonator filled with air. However, LDA is a point-measurement technique, that is, it measures velocity at one spatial location at a time and is not capable of simultaneously mapping the flow in a two-dimensional region.

The measured velocity field inside a standing-wave resonator is the superposition of acoustic and streaming velocities. The magnitude of the acoustic velocity is typically several times larger than that of the streaming velocity. In fact, acoustic velocity is a first order quantity whereas streaming velocity is a second order one. As a result, in a given velocity

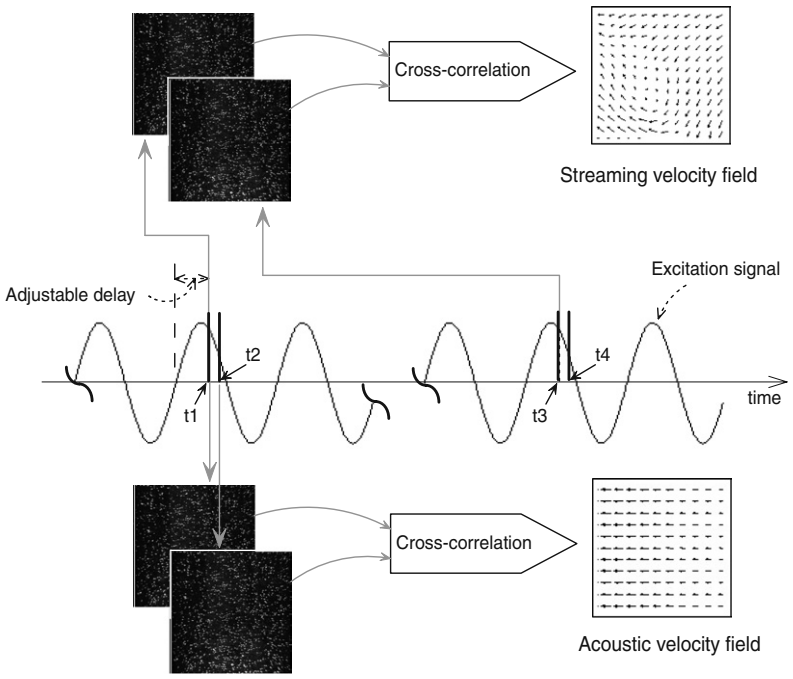

Figure 1. The triggering sequence that shows how the acoustic and streaming velocity fields at a particular phase of the excitation signal are extracted. t_1 to t_4 are the times at which the laser light sheet is pulsed and the flow field is imaged.

measurement, the streaming velocity component is suppressed by the acoustic velocity component. The streaming velocity can be obtained by either removing the acoustic velocity component or doing the velocity measurement in a location where the acoustic velocity is negligible. As the literature review indicates, all of the reported PIV measurements of streaming velocity fields have been done in the vicinity of a velocity node, at which the amplitude of the acoustic velocity is almost zero. In order to measure the streaming velocity fields at different locations along the resonator, it is necessary to find a way to remove the acoustic velocity component. In the present study, we used a synchronized PIV technique that allows us to measure streaming velocities in any spatial region along the resonator and also in the presence of standing waves of significant intensity.

2. Synchronized PIV technique

In the PIV technique, a laser light sheet is pulsed twice with a known time separation between the two pulses. A CCD camera captures the images of the tracer particles at each pulse in the flow field of interest. The displacements of particles between two images are computed by cross-correlating the interrogation region in the first image with the corresponding search region in the second image. The displacement of particles divided by the time separation between the laser pulses provides the velocity field. In the conventional PIV setup, the laser pulses are synchronized with the camera frames. Typically these signals are not synchronized with any flow characteristics as for steady flows it is not necessary. However, for velocity measurements in the presence of an acoustic standing wave, these signals are synchronized with the excitation signal to capture the sequence of velocity fields at the given phase [6].

In this study, we have presented a scheme to simultaneously measure acoustic and streaming velocity fields at a given wave phase using the synchronized PIV technique. The triggering sequence used to sample velocity fields at a particular phase of the excitation signal in this scheme is shown in figure 1. Consider the image taken at time t_1 in figure 1 as the first image and the image taken at time t_2 as the second image, with the time separation of $t_2 - t_1$. The cross-correlation of this image pair provides the acoustic velocity field at time t_1. Now consider the image taken at time t_1 as the first image and the image taken at time t_3 as the second image, with the time separation of $t_3 - t_1$. Since the images acquired at t_1 and t_3 are exactly at the same phase, the acoustic velocity components at these times will be the same and, therefore, the particle shift between these two images will only be due to streaming velocity. Thus, the cross-correlation of this image pair will provide the streaming velocity field at time t_1. Hence, by using this novel approach, both acoustic and streaming velocity fields can be obtained simultaneously at any wave phase.

We developed an electronic circuit to generate a trigger signal which could synchronize the laser pulses and camera frame with any particular phase of the excitation signal. This phase can be adjusted from 0 to 2π and therefore covers the whole period of the excitation waveform. The block diagram and the output waveforms of each block of the synchronization circuit are shown in figure 2. The excitation voltage (TP1) which is used to excite the standing wave inside the tube is sent to the sync generator to produce a rectangular wave synchronized with the zero crossing points of the excitation signal (TP2). The delay generator provides a train of pulses

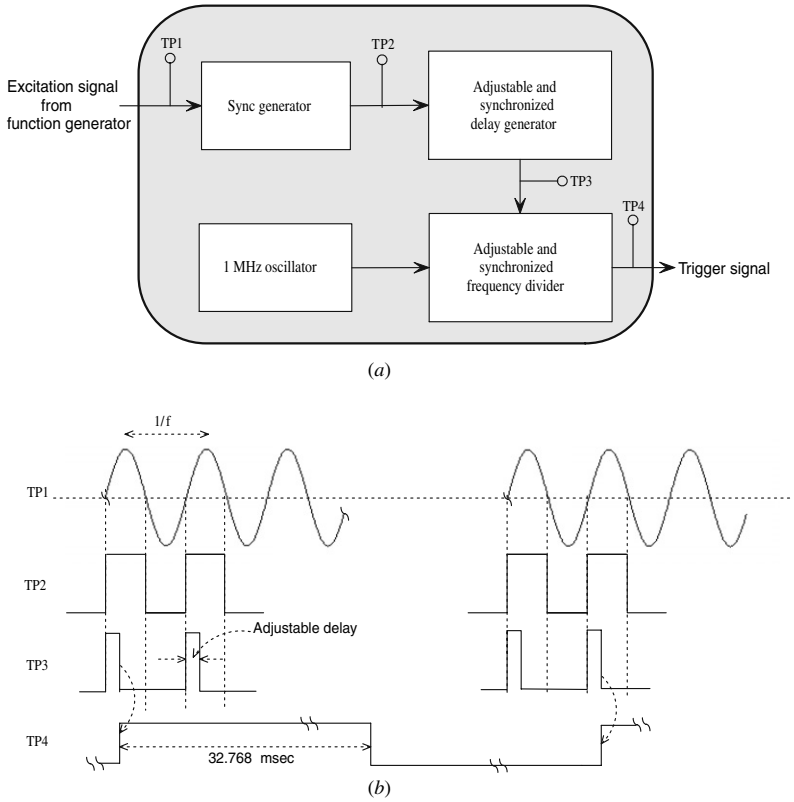

Figure 2. (*a*) Block diagram of the synchronization circuit, and (*b*) the waveforms at different test points (TP) of the synchronization circuit.

with adjustable duty cycle (TP3) which is synchronized with the rising edge of TP2. The rising edge of the trigger output signal (TP4) is synchronized with the falling edge of TP3. By adjusting the duty cycle of TP3, we can select the phase at which PIV images have to be acquired. In the conventional PIV setup, a fixed unsynchronized 15 Hz signal is used as a trigger for both laser and camera. However, in the present synchronized PIV technique, TP4 is used to trigger both laser and CCD camera of the PIV system. That is, both the laser and the camera are synchronized with the acoustic signal via TP4. Although the high state duration of TP4 is fixed (32.768 ms), the low state duration is not fixed because the rising edge of TP4 is synchronized with the excitation signal. Therefore, the frequency of TP4 is not exactly but close to 15 Hz and it is automatically adjusted according to the excitation frequency. For example, the frequency of TP4 for the excitation frequency of 1000 Hz is 15.15 Hz and for 1330 Hz is 15.11 Hz. The frame rate of the camera is twice the frequency of TP4. Furthermore, we can measure the streaming velocity field at any arbitrary excitation frequency because the acoustic frequency is not forced to be a multiple of the frame rate. Rather, the frame rate is forced to be an exact divisor of the acoustic frequency. For a given acoustic frequency, the frame rate is automatically adjusted to a frequency close to 30 Hz. Since the time delay, the width of the trigger signal (TP4), the frequency of the excitation signal and the time separation between two laser pulses are accurately known, the phase where two laser pulses are located in the excitation signal can be calculated.

3. Experimental setup

The experimental setup developed to measure the streaming velocity fields inside the standing-wave tube is shown in figure 3. The acoustic chamber is a Plexiglas channel of square cross-section. The inner cross-section of the channel is 7 cm × 7 cm. The walls of the channel are 6 mm thick. The two-dimensional velocity fields inside the channel were measured using PIV. The measurements were made in a plane parallel to the channel length at the mid-channel location as shown in figure 3. A New Wave Research 120 mJ Nd:YAG laser was used as a light source for the PIV measurements. A digital 2 megapixel progressive scan CCD camera (JAI CV-M2) with the resolution of 1600 × 1200 pixels was used to image the flow. The camera was connected to a PC equipped with a frame grabber (DVR Express, IO Industries, London, ON, Canada) that acquired 8 bit images at a rate of 30 Hz. A four-channel digital delay generator (555-4C, Berkeley Nucleonics Corporation, San Rafael, CA) was used to control the timing of the laser pulses. Bis(2-ethylhexyl) sebacate mist with a mean diameter of 0.5 μm was used as the tracer particles. An aerosol generator (Lavision Inc., Ypsilanti, MI) was used to generate the mist. The acoustic pressure was monitored by a condenser microphone cartridge Model 377A10 PCB Piezotronics. The microphone consists of a microphone cartridge and a microphone preamplifier. A preamplifier Model 426B03 was used in order to measure the sound pressure level. The cartridge screws directly onto the preamplifier housing. The frequency response is almost flat between 5 Hz and 100 kHz. During velocity measurements, the microphone was placed inside a hole in the adjustable

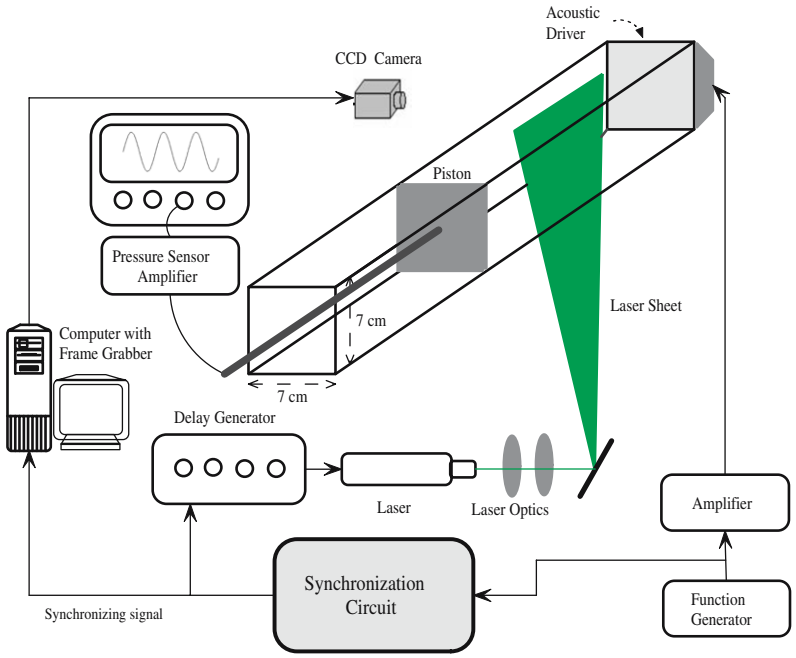

Figure 3. Schematic of the experimental setup and instrumentation.

piston and flashed with the piston inner surface (see figure 3). Thus, the microphone and piston are always at the same position, i.e. at the pressure antinode, and the microphone measures the maximum pressure. A special loudspeaker driver is used to excite the acoustic standing wave inside the tube. The driver has a diaphragm of diameter 51 mm, maximum power of 200 W and dc resistance of 8 Ω. The use of a loudspeaker driver as an acoustic source makes it easy to vary the frequency and intensity of excitation continuously and precisely. A function generator model Agilent 33120A was used to generate the sinusoidal wave of different frequencies and amplitudes. The accuracy of the generated frequency and amplitude are 1 μHz and 0.1 mV, respectively. The signal from the function generator was amplified by a 220 W amplifier (Pioneer SA-1270). The loudspeaker was driven by this amplified signal (see figure 3). The driver frequency was set equal to 1400 Hz. The wavelength (λ) of the acoustic standing wave corresponding to this frequency is 24.5 cm. The length of the channel was adjusted with the movable piston to allow the formation of two full standing waves inside the channel. The acoustic driver produced acoustic wave with the pressure amplitude of $P_0 = 897$ Pa at the pressure antinode. To confirm that the assumption of rigid walls holds for the channel we used in this study, we measured the wall vibration using a Brüel and Kjær laser vibrometer. The maximum wall displacement was found to be approximately 1 μm. This is about 0.5% of the maximum displacement of the acoustic driver which was 200 μm. Thus, we concluded that the wall vibration has no significant effect on the acoustic streaming. The field of view of the CCD camera was set in a way to map the flow field in the half wavelength section. That is, the field of view of the camera was set equal to 12.9 cm horizontally and 9.7 cm vertically. All experiments were conducted in air at 25 °C. The properties of air at this condition are $c_0 = 344$ m s^{-1}, $\rho_0 = 1.29$ kg m^{-3} and $\nu = 1.56 \times 10^{-5}$ m^2 s^{-1}.

As mentioned earlier, mist is used as the tracer particles for PIV measurements. An important issue related to the tracer particles is their response time. That is, how quickly the particles respond to any change in the flow behaviour. In the present study, the density of the tracer particles is much higher than that of air; therefore, it is important to find the response time of the particles. Furthermore, as the particles oscillate under the action of the standing wave, this issue becomes even more critical. The characteristic response time of the seed particles is computed by

$$T_p = u_T/g, \tag{1}$$

where T_p is the particle response time, u_T is the particle terminal velocity and g is the acceleration due to gravity [7]. The terminal velocity is computed by

$$u_T = \frac{(\gamma - 1)D^2 g}{18\nu}, \tag{2}$$

where D is the diameter of the tracer particles, ν is the kinematic viscosity of the fluid and γ is the ratio of the density of particle to the density of fluid [8]. Using the above equations, for $D = 0.5$ μm, $u_T = 6.5$ μm s^{-1} and the particle response time is found to be $T_p = 0.67$ μs. For the driver frequency of 1400 Hz, the particle response is more than 1000 times faster than the time period. Thus, we conclude that the tracer particles accurately follow the flow.

Although for the measurement of streaming velocity vectors, the separation time between two images is about 1/15 s ($t_3 - t_1$ in figure 1), for the acoustic velocity measurement, the separation time between two images ($t_2 - t_1$ in figure 1) must be adjusted appropriately. Due to the oscillation of the particles, the time separation between the two images of an image pair should be much less than a quarter of the time period. Otherwise, the particle displacement computed by cross-correlating the PIV images will be smaller than the actual displacement of the particles. This will result

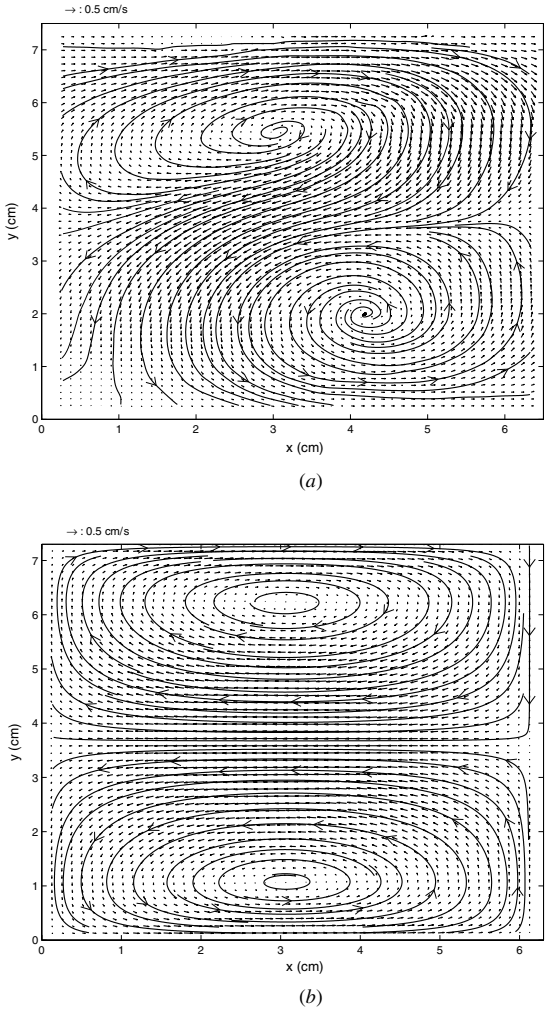

Figure 4. Instantaneous streaming velocity fields for the excitation frequency of 1400 Hz and node pressure of 897 Pa ($R_s = 20.3$) in quarter of the wavelength at time $t/T = 0.9134$, where T is the period of the excitation sinusoidal signal. $x = 0$ correspond to the velocity node and $x = 6.125$ cm correspond to the velocity anti-node at $\lambda/4$: (a) experimental and (b) theoretical.

in underestimated acoustic velocities. On the other hand, for very short separation time, the particle displacement will be too small, which will significantly increase the uncertainty in the velocity measurements. In the present case, the time separation was set equal to 50 μs, which is about four times smaller than the quarter wave period. The vertical dimension of the camera field of view was larger than the channel height. Therefore, before computing the velocity vectors, the images were preprocessed to chop off the regions outside the channel. For PIV cross-correlation, the size of the interrogation region was set equal to 32×32 pixels and the size of the search region was set equal to 64×64 pixels. A 50% window overlap was used in order to increase the nominal resolution of the velocity field to 16×16 pixels. A three-point Gaussian sub-pixel fit scheme was used to obtain the correlation peak with sub-pixel accuracy.

For each set of measurements, 200 PIV images were captured. From these images, 100 acoustic velocity fields and 50 streaming velocity fields were computed using the technique described in section 2. A scheme was used to identify the spurious velocity vectors and then correct them using a local median test [9]. By adjusting the duty cycle of TP3 in figure 2, the measurements have been done at 20 different phases of the excitation signal.

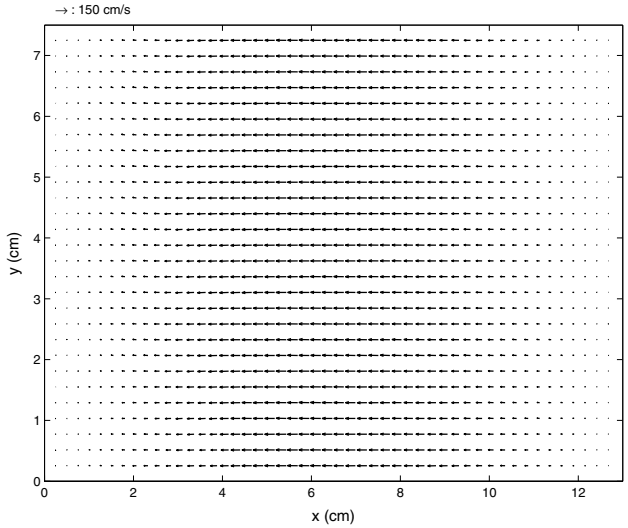

Figure 5. Experimental instantaneous acoustic velocity vectors for the excitation frequency of 1400 Hz and the node pressure of 897 Pa at time $t/T = 0.9134$. $x = 0$ and $x = 12.25$ cm correspond to the velocity nodes and $x = 6.125$ cm correspond to the velocity anti-node. Note that the resolution of the velocity vectors was reduced to half in the plot for better visualization.

4. Results

To confirm that the velocities obtained from the given approach are accurate, the velocity characteristics from the experimental data were compared with those obtained from the analytical solution of the linear wave equation. The amplitude of the axial component of the acoustic velocity field in the linear case is given as

$$u = u_1 \sin(2\pi x/\lambda), \tag{3}$$

where $u_1 = P_0/\rho_0 c_0$ and x is the axial coordinate. The axial component (u_{st}) and transverse component (v_{st}) of the streaming velocity field are

$$u_{st} = \frac{3}{8}\frac{u_1^2}{c}\left(1 - \frac{2y^2}{H^2}\right)\sin(\pi x/\ell), \tag{4}$$

$$v_{st} = -\frac{3}{8}\frac{u_1^2}{c}\frac{2\pi y}{\lambda}\left(1 - \frac{y^2}{H^2}\right)\cos(\pi x/\ell), \tag{5}$$

where y is the transverse coordinate ($-H \leqslant y \leqslant H$), $2H$ is the height of the tube and $\ell = \lambda/4$ [5].

The experimental and theoretical instantaneous streaming velocity vectors in quarter of the wavelength in which the acoustic velocity varies from zero at the velocity node ($x = 0$) to the maximum at $x = \lambda/4 = 6.125$ cm are shown in figure 4. The streamlines are also depicted in figure 4 for better flow visualization. The plot shows that present scheme captures the streaming velocity fields very well. As expected all 50 measurements of the streaming velocity at this phase are consistent and all streaming velocity fields at different phases are quite similar. The instantaneous two-dimensional acoustic

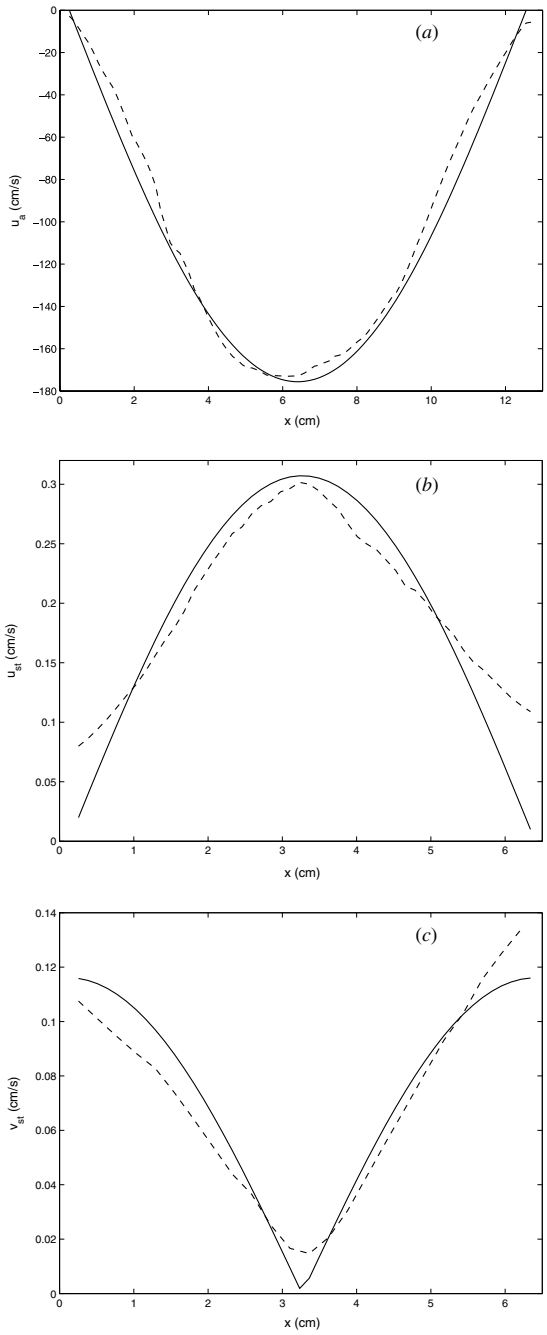

Figure 6. The theoretical (solid line) and experimental (dashed line) values of (*a*) mean acoustic velocity (u_a), (*b*) RMS u_{st} and (*c*) RMS v_{st}, along the resonator for the excitation frequency of 1400 Hz and the node pressure of 897 Pa at time $t/T = 0.9134$. The RMS streaming velocities are computed from the upper vortex in figure 4(*a*).

velocity vectors for this case over half of the wavelength are shown in figure 5. The plot as expected shows the maximum acoustic velocity at the velocity anti-node located at $x = \lambda/4$.

To evaluate the performance of the present approach, the theoretical and experimental values of the mean acoustic velocity and root-mean-square (RMS) streaming velocities along the resonator are quantitatively compared in figure 6. To compute the RMS streaming velocity, the velocity data at each axial location were extracted in the region

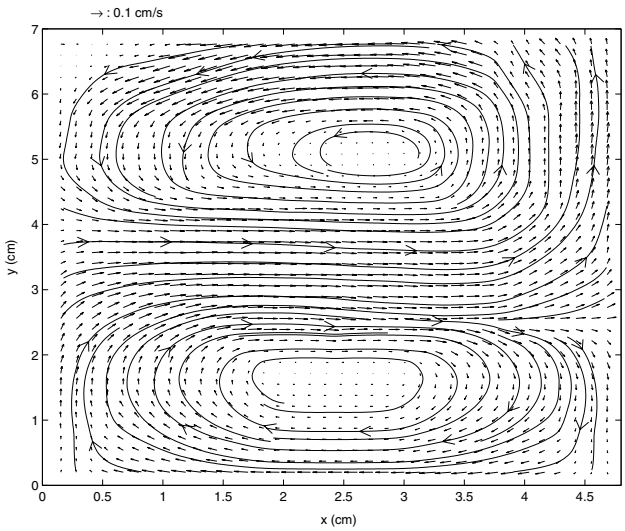

Figure 7. Instantaneous streaming velocity field for the excitation frequency of 1852 Hz and the node pressure of 431 Pa ($R_s = 4.2$) in quarter of the wavelength at time $t/T = 0.038$. $x = 0$ correspond to the velocity node and $x = 4.6$ cm correspond to the velocity anti-node at $\lambda/4$.

occupied by one streaming vortex and the RMS velocity at each axial location was computed from these data. Figure 6 shows that the magnitudes of the streaming velocities are considerably smaller than the magnitudes of the horizontal acoustic velocities, which is also reported by Thompson *et al* [5]. The plot also shows that the variation of the axial and transverse components of the streaming velocity with respect to the axial coordinate is sinusoidal. Good agreement between the theoretical and experimental results for both acoustic and streaming velocities proves the ability of the present method to measure acoustic and streaming velocities simultaneously and accurately at any phase of the acoustic standing wave.

To further confirm that the present approach could accurately extract the streaming velocity fields at different acoustic frequencies and amplitudes, we conducted the experiments at the excitation frequency of 1852 Hz and the pressure amplitude of 413 Pa at the pressure antinode. The streaming velocity field in quarter of the wavelength for this case is shown in figure 7. The streaming velocity patterns are in good agreement with the theoretical ones. The RMS streaming velocities along the resonator for the given case are depicted in figure 8. The corresponding theoretical profiles are also plotted for comparison. Good agreement between the experimental and theoretical profiles confirms that the present scheme can be used under different conditions and that the synchronized PIV technique correctly captured the streaming velocity fields.

The streaming velocity fields in the higher pressure amplitude case (i.e. figure 4(*a*)) show an asymmetry in the streaming vortices, whereas for the lower pressure amplitude case (i.e. figure 7), the asymmetry in the streaming vortices is not very significant. The classical streaming velocity field (figure 4(*b*)) shows symmetric vortices about the centreline of the resonator. The observed asymmetry in the streaming vortices can be explained on the basis of the streaming Reynolds number defined as $R_s = 3u_1^2 H/4c_0\nu$. Yano [10, 11] has shown that the symmetry in the flow pattern of acoustic

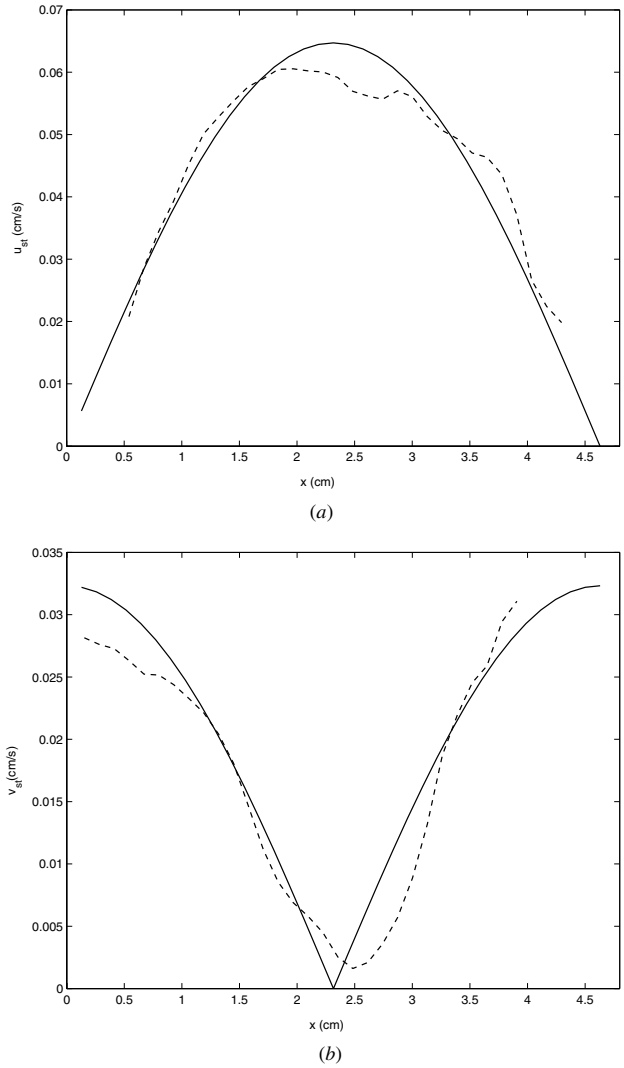

Figure 8. The theoretical (solid line) and experimental (dashed line) values of (*a*) RMS u_{st} and (*b*) RMS v_{st}, along the resonator for the excitation frequency of 1852 Hz and the node pressure of 431 Pa ($R_s = 4.2$) in quarter of the wavelength at time $t/T = 0.038$. The RMS streaming velocities are computed from the upper vortex in figure 7.

streaming is lost when the streaming Reynolds number is moderately large ($R_s \gg 1$), even before the transition to turbulence, whereas for the classical streaming ($R_s < 1$) excited by the linear standing wave, the flow patterns are symmetric. He has also shown that for moderately large values of R_s, the streaming patterns are almost stationary and time invariant [12]. The streaming Reynolds number for the higher pressure amplitude case is $R_s = 20.3$ and for the lower pressure amplitude case is $R_s = 4.2$. As the $R_s = 4.2$ case is close to the classical streaming Reynolds number, the streaming vortices are almost symmetric. As R_s increases, the streaming vortices become more asymmetric as shown in figure 4(*a*).

5. Conclusions

Simultaneous measurement of the acoustic and streaming velocity vectors along a resonator was investigated. A novel approach was used for extracting the streaming velocity fields. In this approach, the velocity fields were sampled at a certain phase of the excitation signal. This phase can be adjusted to cover the whole period of the excitation waveform. Despite all reported PIV measurements of streaming in which the measurements have been done in the vicinity of the velocity node (where acoustic velocities are almost zero), the present technique enables the measurement of the streaming velocities at any location along the standing wave resonator in the presence of large amplitude acoustic waves. The results show that the given approach accurately captures the structure of the streaming velocity fields. The results also show an asymmetry in the streaming vortices at the higher streaming Reynolds number. The comparison of the experimental values of the mean acoustic velocity and RMS streaming velocities with the theoretical ones for two different excitation amplitudes and frequencies confirmed the accuracy of the present approach.

Acknowledgments

This research is funded by grants from the Natural Science and Engineering Research Council of Canada (NSERC) and Concordia University.

References

[1] Boluriaan S and Morris P J 2003 Acoustic streaming: from Rayleigh to today *Int. J. Aeroacoust.* **2** 255–92
[2] Arroyo M P and Greated C A 1991 Stereoscopic particle image velocimetry *Meas. Sci. Technol.* **2** 1181–6
[3] Hann D B and Greated C A 1997 The measurement of flow velocity and acoustic particle velocity using particle image velocimetry *Meas. Sci. Technol.* **8** 1517–22
[4] Campbell M, Cosgrove J A, Greated C A and Rockliff J D 2000 Review of LDA and PIV applied to the measurement sound and acoustic streaming *Opt. Laser Technol.* **32** 629–39
[5] Thompson M W and Atchley A A 2005 Simultaneous measurement of acoustic and streaming velocities in a standing wave using laser Doppler anemometry *J. Acoust. Soc. Am.* **117** 1828–38
[6] Shin Y, Jaewon C and Domoto G A 2005 Compressible flow of liquid in a standing wave tube *J. Fluid Mech.* **536** 321–45
[7] Snyder W H and Lumley J L 1971 Some measurements of particle velocity autocorrelation functions in a turbulent flow *J. Fluid Mech.* **48** 41–71
[8] Siegel D A and Plueddemann A J 1991 The motion of a solid sphere in an oscillating flow: an evaluation of remotely sensed Doppler velocity estimates in the sea *J. Atmos. Ocean. Technol.* **8** 296–304
[9] Siddiqui M H K, Loewen M R, Richardson C, Asher W E and Jessup A T 2001 Simultaneous particle image velocimetry and infrared imagery of microscale breaking waves *Phys. Fluids* **13** 1891–903
[10] Yano T 2005 Numerical simulation of formation of asymmetric acoustic streaming in resonators *58th Ann. Meeting of the Division of Fluid Dynamics (American Physical Society, Chicago, IL, USA, 20–22 November)*
[11] Yano T 2006 Numerical study of high Reynolds number acoustic streaming in resonators *17th Int. Symp. on Nonlinear Acoustics (AIP Conf. Proc.* ***838****)* pp 379–86
[12] Yano T 1999 Turbulent acoustic streaming excited by resonant gas oscillation with periodic shock waves in a closed tube *J. Acoust. Soc. Am.* **106** L7–12